Article

NMR Studies of the Dynamics of a Bifunctional Rhodamine Probe Attached to Troponin C

Olivier Julien, Pascal Mercier, Leo Spyracopoulos, John E. T. Corrie, and Brian D. Sykes

J. Am. Chem. Soc., **2008**, 130 (8), 2602-2609 • DOI: 10.1021/ja0772694

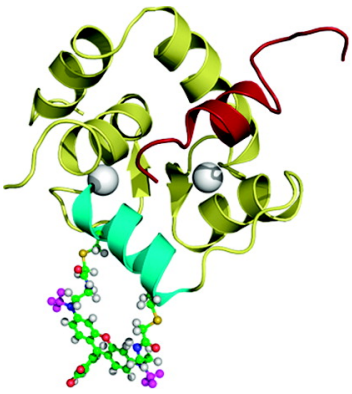

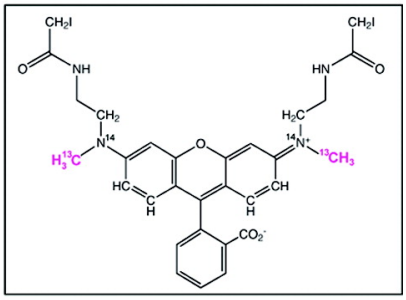

More About This Article

Additional resources and features associated with this article are available within the HTML version:

- Supporting Information
- Links to the 1 articles that cite this article, as of the time of this article download
- Access to high resolution figures
- Links to articles and content related to this article
- Copyright permission to reproduce figures and/or text from this article

View the Full Text HTML

J|A|C|S
ARTICLES
Published on Web 02/02/2008

NMR Studies of the Dynamics of a Bifunctional Rhodamine Probe Attached to Troponin C

Olivier Julien,[†] Pascal Mercier,[†] Leo Spyracopoulos,[†] John E. T. Corrie,[‡] and Brian D. Sykes*,[†]

Department of Biochemistry, University of Alberta, Edmonton T6G 2H7, Canada and the MRC National Institute for Medical Research, The Ridgeway, Mill Hill, London NW7 1AA, United Kingdom

Received September 19, 2007; E-mail: brian.sykes@ualberta.ca

Abstract: Fluorescence polarization measurements of bifunctional rhodamine (BR) probes provide a powerful approach to determine the in situ orientation of proteins within ordered complexes such as muscle fibers. For accurate interpretation of fluorescence measurements, it is important to understand the probe dynamics relative to the protein to which it is attached. We previously determined the structure of the N-domain of chicken skeletal troponin C, BR-labeled on the C helix, in complex with the switch region of troponin I, and demonstrated that the probe does not perturb the structure or dynamics of the protein. In this study, the motion of the fluorescence label relative to the protein has been characterized using NMR relaxation measurements of ^{13}C-labeled methyl groups on the BR probe and ^{15}N-labeled backbone amides of the protein. Probe dynamics were monitored using off-resonance ^{13}C-$R_{1\rho}$, ^{13}C-R_1 and $\{^1H\}-^{13}C$ NOE at magnetic field strengths of 500, 600, and 800 MHz. Relaxation data were interpreted in terms of the overall rotational correlation time of the protein and a two-time scale model for internal motion of the BR methyl groups, using a numerical optimization with Monte Carlo parameter error estimation. The analysis yields a 1.5 ± 0.4 ps correlation time for rotation around the three-fold methyl symmetry axis, and a 0.8 ± 0.4 ns rotational correlation time for reorientation of the $^{13}C-^{14}N$ bond with an associated S^2_s of 0.79 ± 0.03. Order parameters of the backbone NH vectors in the helix to which the probe is attached average $S^2 \approx 0.85$, implying that the amplitude of independent reorientation of the BR probe is small in magnitude, consistent with results from fluorescence polarization measurements in reconstituted muscle fibers.

Introduction

Fluorescent labeling of proteins is a widely used approach for studying the properties of biological systems that range from isolated proteins to intact supramolecular assemblies within live cells. Many applications involve imaging or qualitative analysis, whereas others involve techniques like fluorescence resonance energy transfer (FRET) that can yield quantitative intermolecular distances. However, in very few of these applications has there been a detailed characterization of the three-dimensional (3D) structure of the labeled protein, or the environment and dynamics of the fluorescent label, yet it is evident from many examples that extrinsic fluorescence probes do make interactions with proteins to which they are covalently or noncovalently bound. Information on these interactions is therefore of general interest for better understanding of the use of fluorescence probes. To illustrate the point, an example where structural data are available can be found in a mutant phosphate-binding protein labeled with a particular coumarin fluorophore.[1] Binding of inorganic phosphate to this labeled protein is accompanied by a large fluorescence enhancement, and the crystallographic structure shows the coumarin specifically bound in a hydrophobic pocket that is created as the protein folds around the phosphate ligand.[2] In another recent example, as yet without structural information, we have described two fluorescent sialosides that bind to hemagglutinin.[3] Both ligands undergo changes in fluorescence intensity upon binding, and the binding affinity increases by 3 orders of magnitude compared to that for sialic acid itself, implying that there must be additional interactions between the fluorophores and the protein. Many other such examples exist, but without structural and dynamic information on these interactions, progress in understanding the effects is necessarily limited.

The present work relates to the probe dynamics in fluorescence polarization measurements of bifunctional rhodamine-labeled proteins to determine the in situ orientation of protein domains whose structures are known in vitro. This approach has been used to determine the orientations of domains of myosin regulatory light chain,[4,5] and troponin C[6,7] proteins

[†] University of Alberta.
[‡] National Institute for Medical Research.

(1) Brune, M.; Hunter, J. L.; Howell, S. A.; Martin, S. R.; Hazlett, T. L.; Corrie, J. E. T.; Webb, M. R. *Biochemistry* **1998**, *37*, 10370−10380.
(2) Hirshberg, M.; Henrick, K.; Haire, L. L.; Vasisht, N.; Brune, M.; Corrie, J. E. T.; Webb, M. R. *Biochemistry* **1998**, *37*, 10381−10385.
(3) Munasinghe, V. R. N.; Corrie, J. E. T.; Kelly, G.; Martin, S. R. *Bioconjugate Chem.* **2007**, *18*, 231−237.
(4) Corrie, J. E. T.; Brandmeier, B. D.; Ferguson, R. E.; Trentham, D. R.; Kendrick-Jones, J.; Hopkins, S. C.; van der Heide, U. A.; Goldman, Y. E.; Sabido-David, C.; Dale, R. E.; Criddle, S.; Irving, M. *Nature* **1999**, *400*, 425−430.

10.1021/ja0772694 CCC: $40.75

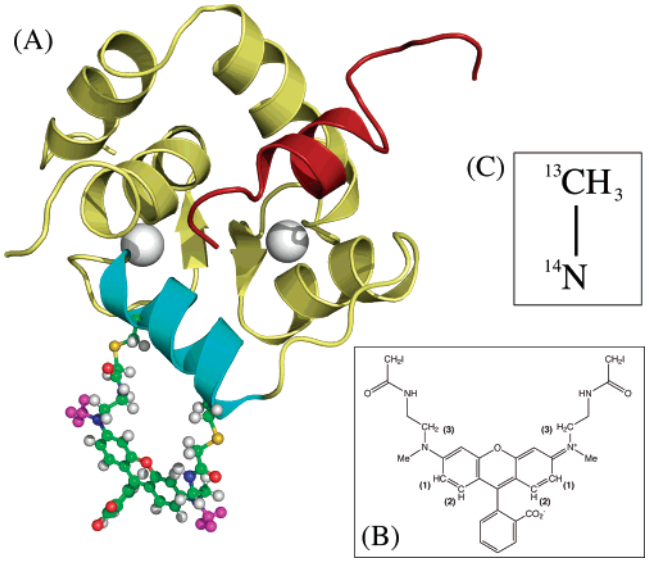

Figure 1. (A) Structure of the molecular complex sNTnC·2Ca^{2+}·$TnI_{115-131}$·BR_{56-63} with the main chain atoms from $sNTnC_{1-90}$ and $sTnI_{115-131}$ colored yellow and red, respectively, and shown in the cartoon representation with Ca^{2+} ions colored white, and the BR probe (attached to residues E56C and E63C of sNTnC) shown in the ball and stick representation with atoms colored as follows: N blue, O red, H white, C green, S yellow, and the ^{13}C-labeled methyl groups in magenta. (B) Chemical structure of the BR probe. The labeled protons correspond to the NOEs identified in Figure 2D. (C) Isotopic labeling of the two methyl groups from the BR probe.

reconstituted into skeletal muscle fibers. BR labeling involves covalent attachment of the probe to two points of the protein via cysteine residues introduced at known positions in the structure (Figure 1). The order parameter $\langle P_{2d} \rangle$ extracted from the polarization data gives information on the amplitude of rapid wobble of the probe on a time scale less than the fluorescence lifetime ($\tau \approx 4$ ns).[8] In previous experiments where BR-labeled troponin C was incorporated into the organized system of a single muscle fiber,[6,7] the measured values of $\langle P_{2d} \rangle$ were in the range 0.87−0.95. These values are consistent with a restricted "wobble-in-a-cone" motion of the probe with a half-angle in the range 19−23°.[8] In the current work, we have made an independent measurement of the dynamics of a bifunctional rhodamine label attached to a mutant (E56,63C) of the N-lobe of chicken skeletal troponin C using NMR relaxation measurements that exploit differential isotope labeling (that is, with ^{13}C on the fluorescence label and ^{15}N labeling of the protein). In contrast to the fluorescence measurements, these measurements were made for the isolated protein in solution so potential probe flexibility would not be influenced by possible protein−protein contacts when the labeled protein is in its native environment of the troponin complex reconstituted into a muscle fiber.

Measurements were made on a complex of the N-domain of skeletal troponin C with a BR probe attached to the C helix, saturated with Ca^{2+}, and bound to the switch peptide of TnI (sNTnC·2Ca^{2+}·$TnI_{115-131}$·BR_{56-63}), for which we have previously determined the structure (Figure 1A) and shown that the structure and dynamics of sNTnC are not affected by the presence of the probe.[9] The rhodamine was ^{13}C-labeled, as shown in Figure 1, B and C, and we compared ^{13}C and ^{15}N NMR relaxation measurements at multiple field strengths of the ^{13}C-labeled BR probe attached to [$U-^{15}$N]troponin C to characterize the motion of the label with respect to the protein. Off-resonance ^{13}C-$R_{1\rho}$, ^{13}C-R_1, and {^{1}H}−^{13}C NOE were measured at 500, 600, and 800 MHz for the ^{13}C-labeled methyl groups of rhodamine within the sNTnC·2Ca^{2+}·$TnI_{115-131}$·BR_{56-63} complex. These measurements allow us to describe and distinguish the motions of the BR probe attached to sNTnC relative to the mobility of troponin C itself in solution and, in conjunction with fluorescence measurements, to interpret the motions of the bifunctional rhodamine label attached to troponin C reconstituted into muscle fibers. The results suggest that there is relatively little motion of the BR probe on a picosecond to nanosecond time scale, in agreement with the fluorescence results. The distribution of probe orientations in fibers shown on a slower time scale[10] may result from motion of the protein domain to which the probe is attached.

Materials and Methods

^{1}H observed, ^{13}C NMR relaxation experiments were performed on 500, 600, and 800 MHz Varian INOVA spectrometers, the last of which was equipped with a cryogenic probe. The BioPack (Varian Inc.) gChsqc pulse sequence[11] was used to record ^{13}C NMR spectra for the R_1 and $R_{1\rho}$ relaxation measurements. We used off-resonance $R_{1\rho}$ measurements as a function of the effective spin-locking field in the rotating frame to disperse the contributions to transverse relaxation from chemical exchange and/or scalar relaxation. R_2 can be calculated by measuring the off-resonance $R_{1\rho}$ and removing the R_1 contribution using the following equations:[12]

$$R_2 = \frac{R_{1\rho}^{obs} - R_1 \cos^2 \theta}{\sin^2 \theta}$$

$$\theta = \arctan\left(\frac{\gamma B_1}{\Delta}\right)$$

where γB_1 is the applied spin-lock field and Δ is the resonance offset from the carrier. The contribution of chemical exchange or scalar interactions to the relaxation can then be determined by measuring R_2 as a function of the strength of the effective spin-locking field in the rotating frame. The off-resonance ^{13}C-$R_{1\rho}$ relaxation rates were measured using different ^{13}C carrier positions (35, 56, and 70 ppm) at three different magnetic fields. The ^{13}C spin-lock rf field strengths (γB_1) were adjusted for magnetic field, relative to the value employed at 600 MHz: γB_1 = 2000 Hz/[(^{1}H frequency in MHz)/600 MHz] (Table 1).

The pulse sequence used for the {^{1}H}−^{13}C NOE experiments was written in-house, based on a similar sequence[13] that was modified to employ pulsed field gradients and ^{1}H spin-lock purge pulses for water suppression. The BioPack (Varian Inc.) gNhsqc pulse sequence[14] was used for measurement of ^{15}N relaxation of [$U-^{15}$N]sNTnC using flip-

(5) Hopkins, S. C.; Sabido-David, C.; van der Heide, U. A.; Ferguson, R. E.; Brandmeier, B. D.; Dale, R. E.; Kendrick-Jones, J.; Corrie, J. E. T.; Trentham, D. R.; Irving, M.; Goldman, Y. E. *J. Mol. Biol.* **2002**, *318*, 1275−1291.
(6) Ferguson, R. E.; Sun, Y. B.; Mercier, P.; Brack, A. S.; Sykes, B. D.; Corrie, J. E. T.; Trentham, D. R.; Irving, M. *Mol. Cell* **2003**, *11*, 865−874.
(7) Sun, Y. B.; Brandmeier, B.; Irving, M. *Proc. Natl. Acad. Sci. U.S.A.* **2006**, *103*, 17771−17776.
(8) Dale, R. E.; Hopkins, S. C.; van der Heide, U. A.; Marszalek, T.; Irving, M.; Goldman, Y. E. *Biophys. J.* **1999**, *76*, 1606−1618.
(9) Mercier, P.; Ferguson, R. E.; Irving, M.; Corrie, J. E. T.; Trentham, D. R.; Sykes, B. D. *Biochemistry* **2003**, *42*, 4333−4348.
(10) Julien, O.; Sun, Y. B.; Knowles, A. C.; Brandmeier, B. D.; Dale, R. E.; Trentham, D. R.; Corrie, J. E. T.; Sykes, B. D.; Irving, M. *Biophys. J.* **2007**, *93*, 1008−1020.
(11) Kay, L. E.; Nicholson, L. K.; Delaglio, F.; Bax, A.; Torchia, D. A. *J. Magn. Reson.* **1992**, *97*, 359−375.
(12) Deverell, C.; Morgan, R. E.; Strange, J. H. *Mol. Phys.* **1970**, *18*, 553−559.
(13) Nicholson, L. K.; Kay, L. E.; Baldisseri, D. M.; Arango, J.; Young, P. E.; Bax, A.; Torchia, D. A. *Biochemistry* **1992**, *31*, 5253−5263.
(14) Kay, L. E.; Keifer, P.; Saarinen, T. *J. Am. Chem. Soc.* **1992**, *114*, 10663−10665.

Table 1. NMR Parameters Used to Acquire the Different ^{13}C Relaxation Experiments at 500, 600, and 800 MHz

experiment (carrier)	spectrometer (MHz)	γB_1 (Hz)	nt	at (s)	d1 (s)	relaxation delay [s]; interval (s)
R_1 (35 ppm)	500	−	1536	0.073	5.0	[0.1−1.7]; (0.2)
	600	−	2048	0.064	5.0	[0.1−1.0]; (0.1)
	800	−	2048	0.085	9.0	[0.1−1.5]; (0.2)
$R_{1\rho}$ (35 ppm)	500	1667	2560	0.073	3.0	[0.1−1.7]; (0.2)
	600	2000	256	0.064	5.0	[0.1−1.0]; (0.1)
	800	2667	2048	0.085	9.0	[0.1−1.5]; (0.2)
$R_{1\rho}$ (56 ppm)	500	1667	2560	0.073	3.0	[0.1−1.7]; (0.2)
	600	2000	2000	0.064	3.0	[0.1−1.0]; (0.1)
$R_{1\rho}$ (70 ppm)	500	1667	2560	0.073	3.0	[0.1−1.7]; (0.2)
	600	2000	3072	0.064	3.0	[0.1−1.0]; (0.1)
{^{1}H}−^{13}C NOE	500	−	8192	0.051	>8.5	−
	600	−	4096	0.051	>8.5	−
	800	−	4096	0.051	>8.5	−

[a] The following Biopak parameters were also used: $\lambda = 0.0011$, tCH = 0.0011, and the sensitivity enhancement was not used.

back pulses for water suppression and a γB_1 of 6.4 kHz for ^{15}N 180° pulses during CPMG. The gnoesyChsqc pulse sequence[15] was used for the acquisition of the 3D ^{13}C NOESY HSQC NMR spectrum. The ^{15}N relaxation rates were measured with 2D {^{1}H−^{15}N}-HSQC spectra, while the ^{13}C relaxation rates were measured from 1D {^{1}H−^{13}C}-HSQC spectra (Table 1). All spectra were acquired at 303 K. The programs NMRPipe[16] and NMRView 5.2.2 (One Moon Scientific Inc.) were used to process and assign the 2D {^{1}H−^{15}N}-HSQCs and the 3D ^{13}C NOESY HSQC. All other spectra were processed and analyzed with VnmrJ v2.1B (Varian Inc.). The intensities of the resonances used to measure the relaxation rates were fitted to a monoexponential decay. The errors reported for the relaxation rates were estimated from the nonlinear least-squares fitting routine within the in-house program xcrvfit.[17] Errors on the NOE were calculated from the signal-to-noise of the respective spectra.

In the absence of other relaxation mechanisms, the R_1, R_2, and NOE values are given by:[18,19]

$$R_1 = Nd^2[J(\omega_H - \omega_C) + 3J(\omega_C) + 6J(\omega_H + \omega_C)] + CJ(\omega_C)$$

$$R_2 = Nd^2[4J(0) + J(\omega_H - \omega_C) + 3J(\omega_C) + 6J(\omega_H + \omega_C)] + 6J(\omega_H) + C\left[\frac{2}{3}J(0) + \frac{1}{2}J(\omega_C)\right] + R_{ex}$$

$$\mathrm{NOE} = 1 + \frac{\gamma_H}{\gamma_C}d^2\left[\frac{N[6J(\omega_H + \omega_C) - J(\omega_H - \omega_C)]}{R_1}\right]$$

where $d^2 = (1/4)(\mu_0/4\pi)[\gamma_H\gamma_C(h/2\pi)]^2(1/r^6_{CH})$ and $C = (\omega_c\,\Delta\sigma)^2/3$, μ_0 is the permittivity of free space, h is Planck's constant, γ_H and γ_C are the gyromagnetic ratios of ^{1}H and ^{13}C, r_{CH} is the ^{1}H−^{13}C distance (1.11 Å), R_{ex} is the contribution from chemical exchange and is assumed to be proportional to ω^2, and $\Delta\sigma$ is the breadth of an axially symmetric ^{13}C CSA. However, the effect of CSA on the calculated relaxation rates was verified to be negligible in the current study (assuming a value of 25 ppm for a methyl ^{13}C). The ^{13}C−^{14}N dipole−dipole contributions to relaxation rates are also small and were neglected.

Relaxation rates were analyzed using a modified model-free approach, separating the fast and slow internal motions of the CH_3 group:[13,20−22]

$$J(\omega) = \frac{2}{5}\left[\frac{S^2\tau_m}{1 + (\omega\tau_m)^2} + \frac{(1 - S^2_f)\tau_1}{1 + (\omega\tau_1)^2} + \frac{S^2_f(1 - S^2_S)\tau_2}{1 + (\omega\tau_2)^2}\right]$$

where τ_m is the overall isotropic rotational correlation time of the protein, S^2_f is the order parameter for the fast rotation of the CH_3 group around the three-fold symmetry axis (equal to 0.111 for ideal tetrahedral geometry[21]), S^2_s is the order parameter for the slower motion ($\tau_s < \tau_m$) of the ^{13}C−^{14}N bond, τ_f and τ_s are the lifetimes of these fast and slow motions, respectively, and

$$S^2 = S^2_f S^2_s, \quad \tau_1^{-1} = \tau_m^{-1} + \tau_f^{-1} \quad \text{and} \quad \tau_2^{-1} = \tau_m^{-1} + \tau_s^{-1}$$

[U−^{15}N]-labeled and [U−^{13}C,^{15}N]-labeled protein were expressed, purified, and BR-labeled as previously described.[9] The NMR sample used for relaxation measurements was prepared as follows: the sNTnC·2Ca^{2+}·TnI$_{115-131}$·BR$_{56-63}$ complex was formed in solution using 0.8 mg of [U−^{15}N]sNTnC·[^{13}C]BR$_{56-63}$, 1 μL of 1 M $CaCl_2$, and 1 mg of sTnI$_{115-131}$ (Ac-RMSADAMLKALLGSKHK-NH_2). The complex was diluted in 300 μL of NMR buffer (90% H_2O/10% D_2O, 250 mM KCl, and 10 mM imidazole), 6 μL protease inhibitor cocktail (Calbiochem), 5 μL of 0.23 M sodium azide, and 20 μL of 5 mM DSS-d_4 for referencing (Chenomx Inc., Canada). A pH of 6.65 was measured from the chemical shift of the imidazole H2 proton.[23] The relatively high salt concentration was necessary to reduce protein dimerization, as previously described.[9] The sample was subsequently diluted 3-fold with NMR buffer to further reduce dimerization and was transferred to a 5 mm Shigemi tube (Shigemi Ltd., Japan). A higher concentration sample containing 3.0 mg of [U−^{15}N,^{13}C]sNTnC·2Ca^{2+}·[^{13}C]BR$_{56-63}$ with excess sTnI$_{115-131}$ was used to acquire a 3D ^{13}C NOESY HSQC NMR spectrum.

Results

The first step in analyzing the dynamics of the BR label attached to sNTnC is characterization of the overall rotational motion of the protein. This step is important, since sNTnC is known to dimerize as the concentration increases. The average backbone amide ^{15}N-R_2 is directly proportional to molecular mass and can be used to evaluate the monomer/dimer ratio of sNTnC in the sNTnC·2Ca^{2+}·TnI$_{115-131}$·BR$_{56-63}$ complex in solution. We used the integral of the amide region from 1D CPMG-based {^{1}H−^{15}N}-HSQC NMR spectra as a function of variable ^{15}N relaxation delays to determine the average ^{15}N-R_2 of the protein. The theoretical ^{15}N-R_2 based upon molecular weight is 8.3 s^{-1} for the monomer,[9] corresponding to an expected macromolecular rotational correlation time of approximately 7.6 ns.[24] The initial concentration of protein (0.3 mM) displayed an ^{15}N-R_2 value of 9.0 s^{-1}, indicating slight dimerization. We then diluted the sample 3-fold with NMR buffer and measured an ^{15}N-R_2 of 8.0 s^{-1}, corresponding to the expected value for monomeric protein. Consequently, this diluted sample was used to perform the ^{13}C relaxation experiments for the BR probe attached to sNTnC.

Figure 2A shows a 1D {^{1}H−^{13}C}-HSQC NMR spectrum of sNTnC·2Ca^{2+}·TnI$_{115-131}$·BR$_{56-63}$, acquired in the absence of ^{13}C decoupling, which allows for a longer acquisition time, results in better signal-to-noise ratio and higher resolution in the spectrum, and allows for measurement of the $^1J_{HC}$ coupling

(15) Zhang, O. W.; Kay, L. E.; Olivier, J. P.; Forman-Kay, J. D. *J. Biomol. NMR* **1994**, *4*, 845−858.
(16) Delaglio, F.; Grzesiek, S.; Vuister, G. W.; Zhu, G.; Pfeifer, J.; Bax, A. *J. Biomol. NMR* **1995**, *6*, 277−293.
(17) http://www.bionmr.ualberta.ca/bds/software/xcrvfit/index.html.
(18) Abragam, A. *The Principles of Nuclear Magnetism*; Clarendon Press: Oxford, 1961.
(19) Lee, A. L.; Flynn, P. F.; Wand, A. J. *J. Am. Chem. Soc.* **1999**, *121*, 2891−2902.
(20) Clore, G. M.; Szabo, A.; Bax, A.; Kay, L. E.; Driscoll, P. C.; Gronenborn, A. M. *J. Am. Chem. Soc.* **1990**, *112*, 4989−4991.
(21) Lipari, G.; Szabo, A. *J. Am. Chem. Soc.* **1982**, *104*, 4546−4559.
(22) Lipari, G.; Szabo, A. *J. Am. Chem. Soc.* **1982**, *104*, 4559−4570.
(23) Sykes, B. D.; Saltibus, L. F.; Spyracopoulos, L. *NMR Newsletter* **1998**, *479*, 11−12.
(24) Spyracopoulos, L.; Gagné, S. M.; Sykes, B. D. In *Dynamics, Structure, and Function of Biological Macromolecules*; Jardetzky O., Finucane, M. D., Eds.; IOS Press: Amsterdam, 2001; pp 37−44.

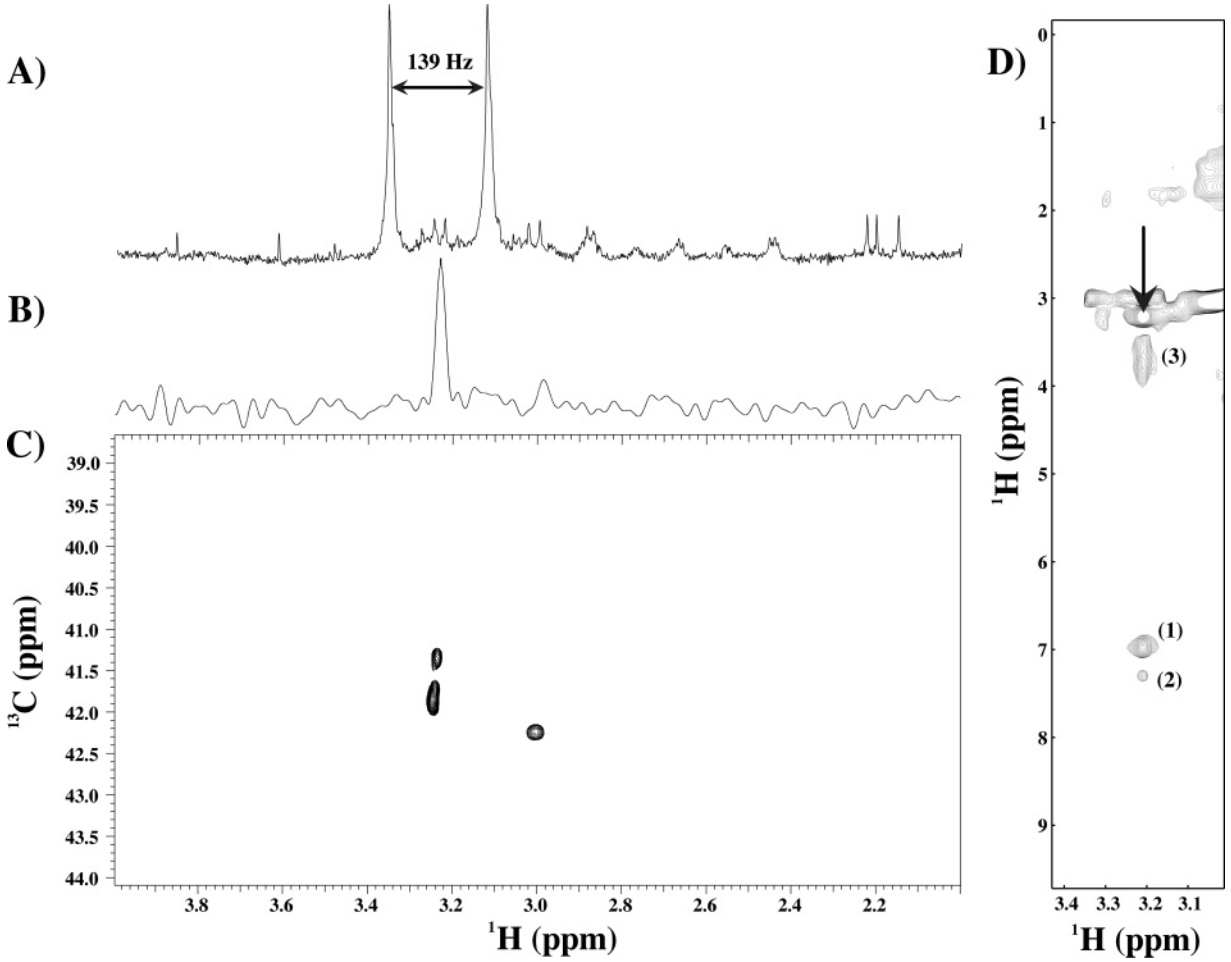

Figure 2. NMR spectra for sNTnC·2Ca^{2+}·TnI$_{115-131}$·BR$_{56-63}$. 1D {^{1}H−^{13}C}-HSQC spectrum for [*U*−^{15}N]sNTnC·2Ca^{2+}·sTnI$_{115-131}$·[^{13}C]BR$_{56-63}$ acquired at 600 MHz in the absence (A) and presence (B) of ^{13}C decoupling. (C) 2D {^{1}H−^{13}C}-HSQC of [*U*−^{15}N]sNTnC·2Ca^{2+}·sTnI$_{115-131}$· [^{13}C]BR$_{56-63}$. (D) ^{13}C plane (41.8 ppm) from a 3D {^{13}C} NOESY HSQC for [*U*−^{15}N,^{13}C]sNTnC·2Ca^{2+}·sTnI$_{115-131}$·[^{13}C]BR$_{56-63}$ acquired at 800 MHz. The peak identified by an arrow corresponds to the diagonal cross-peak, while the numbered cross-peaks are NOEs between the *N*-methyl groups and the protons designated by those labels in Figure 1.

constant for the observed resonances. The two high-intensity peaks with ^{1}H chemical shifts of 3.12 and 3.35 ppm correspond to the two equivalent methyl groups of the BR probe and are separated by $^{1}J_{CH} \approx 139$ Hz. The other narrow peaks in the spectrum arise from natural abundance ^{13}C of excess, unbound sTnI$_{115-131}$ peptide. Figure 2B shows a 1D {^{1}H−^{13}C}-HSQC NMR spectrum in the presence of ^{13}C decoupling, with the methyl resonance(s) at 3.23 ppm. In Figure 2C, the 2D {^{1}H−^{13}C}-HSQC spectrum shows two distinct resonances for the methyl groups with ^{1}H chemical shifts of ∼3.23 ppm, and ^{13}C chemical shifts of 41.3 and 41.8 ppm. These different cross-peaks reflect the presence of the two diastereoisomers that arise because of atropisomerism in the rhodamine structure (see ref[4] for previous discussion), and are consistent with doubling of backbone amide resonances in 2D {^{1}H−^{15}N}-HSQC NMR spectra of the troponin C for residues situated near the attachment points of the rhodamine probe.[9,10] Given that the proton chemical shifts of the methyl resonances are almost identical, these two resonances are not distinguishable in 1D {^{1}H−^{13}C}-HSQC NMR spectra (Figure 2B), and are manifested as weak shoulders on both peaks in the higher-resolution spectrum shown in Figure 2A. Thus, the measured ^{13}C relaxation rates correspond to a combination of two methyl groups from both diastereoisomers. A weak third resonance is seen near 3.0 ppm in Figure 2C, which most likely arises from the ϵCH$_2$ groups of the lysine residues of excess sTnI$_{115-131}$ peptide. This resonance has $^{1}J_{CH} = 142$ Hz, different from the value of 139 Hz for the methyl group of the BR probe.

Figure 2D shows a slice (^{13}C = 41.8 ppm) from a 3D ^{13}C NOESY HSQC NMR spectrum. Cross-peaks identified by particular marks correspond to NOEs between protons of the [^{13}C]methyl groups of the BR probe and other protons within ∼5 Å. For example, the peaks marked (3) correspond to the methylene groups adjacent to the methyl-bearing nitrogen atoms, and those marked (1) and (2) represent the NOEs with the H2′,-H7′ and H1′,H8′ protons respectively, of the xanthene ring (see Figure 1). The weaker NOE to the H1′,H8′ protons likely arises from spin diffusion. The peak identified by an arrow corresponds to the diagonal cross-peak of the methyl groups. The same contacts are observable in the ^{13}C plane at 41.3 ppm. The NOE data are consistent with the conformation of the linker arms between rhodamine and the protein as shown in Figure 1, A and B. Additionally, NOE contacts between the ^{13}C-labeled methyl groups and the protein are not observed, supporting previous results.[9]

To characterize the motion of the BR label, we studied the ^{13}C relaxation of the methyl groups employing indirect detection pulse sequences. Significant errors can be introduced in ^{13}C

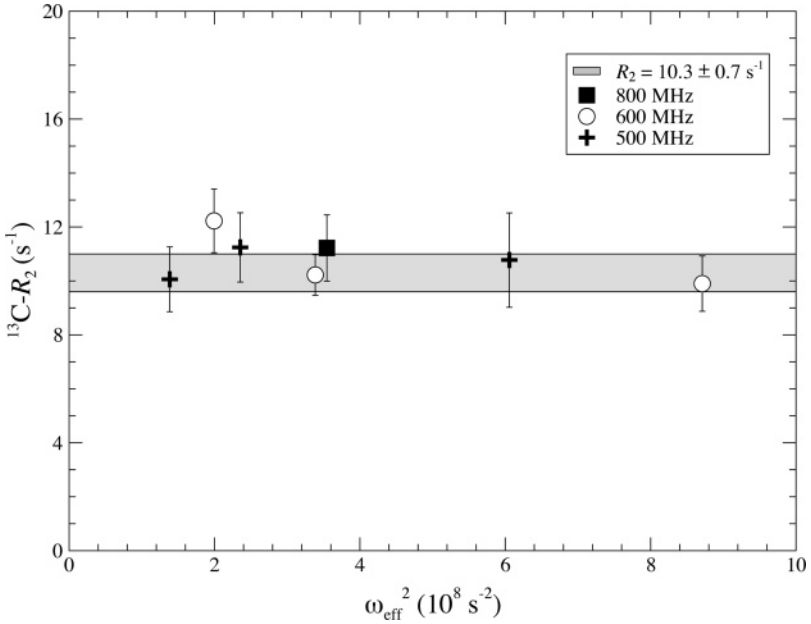

Figure 3. ^{13}C-R_2 values calculated from off-resonance $R_{1\rho}$ measurements of the BR probe as a function of the effective field (ω_{eff}^2) at 303 K. The shaded area indicates $\langle R_2 \rangle \pm 1\sigma$.

relaxation measurements of AX_3 spin systems due to contributions to the relaxation of the ^{13}C nucleus from cross-correlation between $^1H-^{13}C$ dipolar interactions, and between $^1H-^{13}C$ dipolar interactions and ^{13}C CSA. Pulse sequence strategies to minimize these errors have been described elsewhere[13,25,26] and involve adjustment of various timings for standard ^{13}C-R_1 and ^{13}C-$R_{1\rho}$ pulse sequences. Specifically, the refocusing delay τ was chosen to give $2\pi\ ^1J_{CH}\tau = 54.7°$ (0.955 rad), so magnetization from individual ^{13}C transitions is transferred uniformly to ^1H magnetization. The INEPT delay for polarization transfer was set to less than $1/(4J_{CH})$ to minimize relaxation losses during delays. Proton 180° pulses were applied during variable relaxation delays to minimize the effect of differential ^1H relaxation. Sensitivity enhancement was not used in order to reduce the number of delays. The purpose of the experimental modifications noted above is to simplify the interpretation of measured relaxation rates which would otherwise be a more complex mixture of fast and slow relaxation contributions.[27] Under the proper experimental conditions, the initial portion of the relaxation curve is a single-exponential decay corresponding to the fast component of the relaxation. In the present case, it is also possible that there are additional contributions to ^{13}C relaxation due to scalar relaxation involving the attached ^{14}N nucleus (Figure 1C), and chemical exchange broadening from the partial dimerization. In this work, we have used off-resonance $R_{1\rho}$ measurements as a function of the effective spin-locking field in the rotating frame to disperse these contributions to the relaxation.

We first measured the longitudinal ^{13}C-R_1 relaxation rate and the $\{^1H\}-^{13}C$ NOE of the methyl groups (Table 2). The NOE values correspond to the intensity ratio of the methyl group peaks measured with and without ^1H saturation, respectively.

Table 2. Longitudinal ^{13}C Methyl Relaxation Rates and $\{^1H\}-^{13}C$ NOE

spectrometer (MHz)	R_1 (s^{-1})	NOE
500	0.65 ± 0.04	1.5 ± 0.1
600	0.57 ± 0.02	1.5 ± 0.1
800	0.46 ± 0.02	1.5 ± 0.1

We obtained an average NOE of 1.5 ± 0.1 for the BR-probe methyl groups at the three magnetic field strengths. By comparison, the NOE measured for natural abundance methyl groups at 0.89 ppm (arising from excess $sTnI_{115-131}$) is 2.2 ± 0.1 (data not shown), the expected value for methyl groups of a peptide. To measure the ^{13}C-R_2 relaxation rate, off-resonance ^{13}C-$R_{1\rho}$ experiments were performed as a function of the effective spin-locking field in the rotating frame to determine whether scalar and/or exchange-broadening contributions to the transverse relaxation of the methyl groups on the BR probe were significant. The contribution from transverse relaxation was subsequently calculated from the measured off-resonance ^{13}C-$R_{1\rho}$ values. The calculated ^{13}C-R_2 values at 500, 600, and 800 MHz are plotted as a function of the effective field in Figure 3. No significant relaxation dispersion is observed, indicating that contributions from both scalar relaxation and chemical exchange are small.

We analyzed the relaxation data following methodologies described in previous studies.[13,19,28] A numerical optimization approach was used, in conjunction with Monte Carlo parameter error estimation.[29] All of the data at three fields were used for global optimization of the fit by varying the parameters τ_s, τ_f, and S^2_s, with S^2_f assumed to be 0.111. The rotational correlation time of the complex was fixed at 8.3 ns, as reported by Mercier et al.[9] and corroborated by our measurement of the average ^{15}N-R_2 backbone amide relaxation rate. We found that the data were better fit at the lower fields, and the fit improved by including

(25) Kay, L. E.; Bull, T. E.; Nicholson, L. K.; Griesinger, C.; Schwalbe, H.; Bax, A.; Torchia, D. A. *J. Magn. Reson.* **1992**, *100*, 538−558.
(26) Palmer, A. G.; Wright, P. E.; Rance, M. *Chem. Phys. Lett.* **1991**, *185*, 41−46.
(27) Iwahara, J.; Jung, Y. S.; Clore, G. M. *J. Am. Chem. Soc.* **2007**, *129*, 2971−2980.
(28) Ishima, R.; Petkova, A. P.; Louis, J. M.; Torchia, D. A. *J. Am. Chem. Soc.* **2001**, *123*, 6164−6171.
(29) Spyracopoulos, L. *J. Biomol. NMR* **2006**, *36*, 215−224.

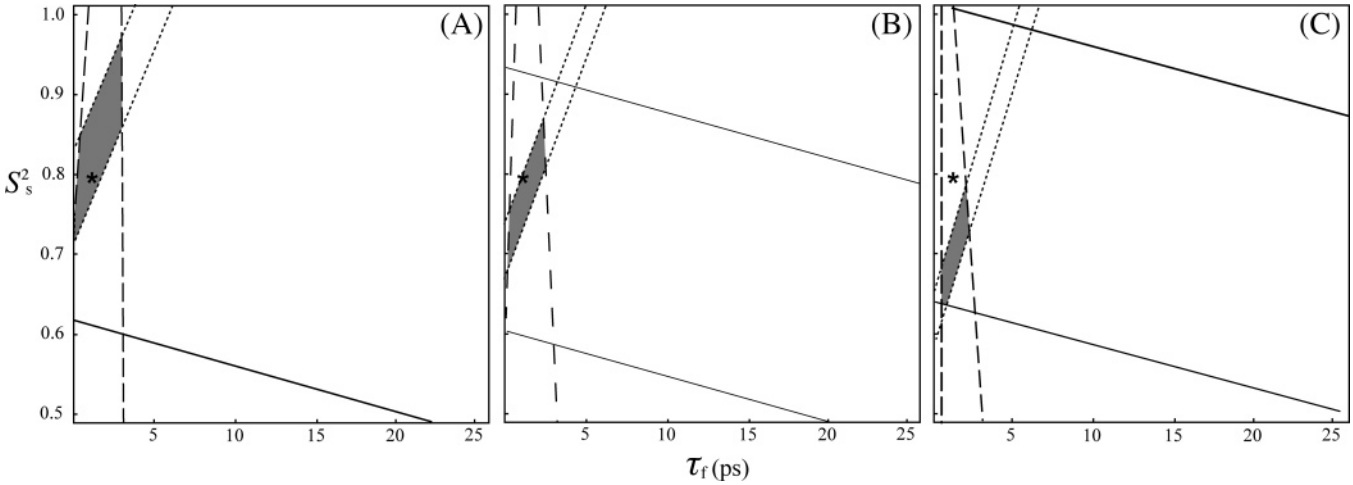

Figure 4. Contour plot showing calculated $R_1 \pm 1.5\sigma$ (···), $R_2 \pm 1.5\sigma$ (−), and NOE $\pm 1.5\sigma$ (---) as a function of S^2_s and τ_f at (A) 500 MHz (B) 600 MHz, and (C) 800 MHz using $\tau_s = 0.8$ ns. The intersections where all of the experimental values are satisfied at each field are colored in gray and the solution from the global optimization is shown with an asterisk.

a R_{ex} term (0.8 s^{-1} at 500 MHz) to compensate for chemical exchange broadening. Using these conditions, we performed 200 Monte Carlo simulations yielding $\tau_f = 1.5 \pm 0.4$ ps, $\tau_s = 0.8 \pm 0.4$ ns, and $S^2_s = 0.79 \pm 0.03$. To visualize how the individual relaxation measurements constrain the fit, contour plots corresponding to the experimental ^{13}C-R_1, ^{13}C-R_2, and NOE at 500, 600, and 800 MHz are shown in Figure 4 as a function of S^2_s and τ_f. The intersections where all of the experimental values are satisfied at each field are colored in gray. Comparison of the three panels allows one to see which values of S^2_s and τ_f satisfy the NMR data observed at all three fields. The global fit is indicated by an asterisk. Figure 4 shows that the R_1 at 800 MHz is just outside ($\sim 2\ \sigma$) of the global fit.

We also looked at the solvent accessibility of the backbone amides of sNTnC·2Ca^{2+}·$TnI_{115-131}$·BR_{56-63}, using hydrogen exchange NMR experiments on a sample similar to the [$U-^{15}$N]-sNTnC·2Ca^{2+}·$TnI_{115-131}$·BR_{56-63} sample but with the complex freshly dissolved in 99.9% D_2O instead of H_2O. A 2D {^{1}H−^{15}N}-HSQC NMR spectrum was acquired for this sample after 2 h and was compared to that of sNTnC·2Ca^{2+}·$TnI_{115-131}$·BR_{56-63} in H_2O (Figure 5). The resonances in blue correspond to the residues protected from exchange with the deuterated solvent. These residues are located in the middle of α-helical secondary structure elements. This is consistent with slower exchange for backbone amides involved in the hydrogen bond network of secondary structure. The presence of the BR probe does not confer additional protection of the amides of helix C over those in other helices or over those in helix C of the wild-type protein, which also exchange within 2 h (data not shown).

Discussion

A quantitative understanding of the dynamics of the BR label is important for the proper use of the fluorescence polarization method for determining orientation of protein domains in situ. When this approach was used to determine the orientation of troponin C in muscle fibers,[6,7] analysis of the fluorescence polarization measurements indicated that the rhodamine label was relatively immobile on a time scale faster than the fluorescence lifetime (~4 ns). This was evidenced by derived order parameters $\langle P_{2d} \rangle$ higher than 0.87 for different attachment sites, including attachment to the C helix.[7] These order parameters imply limited motion of the probe[8] and can be interpreted using the wobble-in-a-cone model with a half-angle of 19−23°. The ^{13}C NMR relaxation measurements presented herein provide an independent estimate of the mobility of the BR label attached to the C helix of troponin C, free of the influence of protein−protein interactions within the thin filament. It is important to note that the fluorescence parameter $\langle P_{2d} \rangle$ is an order parameter, whereas the NMR parameter S^2, often referred to as an order parameter, is actually the square of the order parameter.

^{13}C NMR relaxation measurements for methyl groups are theoretically and experimentally complicated. The relaxation involves cross-correlation between dipolar and CSA mechanisms, in addition to possible contributions from scalar relaxation and chemical exchange. We therefore followed previous recommendations to circumvent adverse effects of cross-correlated relaxation[25,30] and employed off-resonance $R_{1\rho}$ methods to measure accurate relaxation parameters. In addition, we used low protein concentrations to avoid complications arising from partial protein dimerization. The analysis of the ^{13}C relaxation data for the BR CH_3 groups using the rotational correlation time for the protein derived from the ^{15}N relaxation data ($\tau_m = 8.3$ ns) yielded $\tau_f = 1.5 \pm 0.4$ ps, $\tau_s = 0.8 \pm 0.4$ ns, and $S^2_s = 0.79 \pm 0.03$. The value for τ_f is quite short when compared with methyl groups within proteins[31] but is consistent with reduced steric crowding around the sp^2-hybridized nitrogens of the BR probe. The value for τ_s is not well defined, but it does not have any significant effect on the calculated S^2_s.[19] Of particular interest is the derived order parameter S^2_s for the amplitude of spatial fluctuations of the N−CH_3 axis of the BR label. This value is in very close agreement with the squared fluorescence order parameters $\langle P_{2d} \rangle$ ($>0.87^2 = 0.76$), indicating that the motion of the CH_3 groups and the xanthene ring are very similar as expected from the partial double bond character of the aryl-N bond in the resonance-stabilized rhodamine structure. The rotational barrier determined by high-level ab initio calculations[32] for the parent tetramethylrhodamine is 11.8

(30) Massi, F.; Grey, M. J.; Palmer, A. G. *Protein Sci.* **2005**, *14*, 735−742.
(31) Xue, Y.; Pavlova, M. S.; Ryabov, Y. E.; Reif, B.; Skrynnikov, N. R. *J. Am. Chem. Soc.* **2007**, *129*, 6827−6838.
(32) Cavallo, L.; Moore, M. H.; Corrie, J. E. T.; Fraternali, F. *J. Phys. Chem.* **2004**, *108*, 7744−7751.

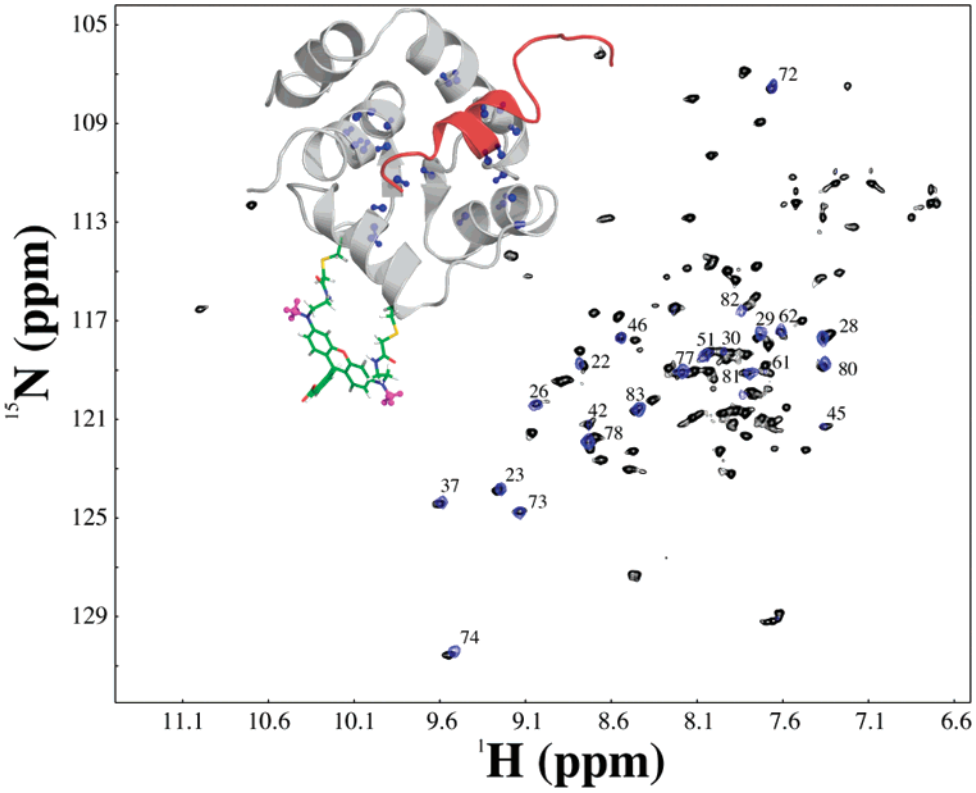

Figure 5. Main chain amide hydrogen exchange for sNTnC·2Ca^{2+}·TnI$_{115-131}$·BR$_{56-63}$. For the superimposed 2D {^{1}H−^{15}N}-HSQC spectra, the black peaks correspond to main chain amides in the complex in 90% H_2O/10% D_2O, and the blue peaks, to slowly exchanging amides that remain after 2 h in 99.9% D_2O. (Inset) Structure of the complex, where amides protected from exchange with solvent are highlighted in blue and labeled with their respective residue number in the spectra.

kcal mol^{-1} and could be expected to be greater in the BR structure because of the linkage to cysteine residues in the protein. The probe cannot be expected to be more rigid than the helix to which it is attached. The order parameters of the backbone amide NH vectors of the C helix are uniform and ~0.85.[33] Consequently, the small difference between the order parameters of the C helix and of the BR probe indicate that the BR probe is virtually immobile relative to the protein.

While this conclusion supports the utility of the overall bifunctional rhodamine approach, it might be considered somewhat surprising. The obvious question is how is the label immobilized, especially considering that it is attached to the protein by several rotatable bonds between the Cys α carbon and the rhodamine N−CH_3 moieties. Possibilities are (1) the fluorophore remains extended from the protein surface and does not move away from its position; (2) the probe is flexible, but the motion is roughly parallel to the N−CH_3 axis and/or the fluorescence excitation dipole moment, and thus the motion is "invisible" to the relaxation and/or fluorescence measurements; or (3) the label is immobilized by hydrophobic contact with the protein surface. The first option seems unreasonable on biophysical grounds, given the flexibility of the linkages to the label. The second option is possible, in whole or in part, given the attachment to two parallel residues on a helix. The third option is supported by molecular dynamics calculations which suggest that the probe forms an interaction with the protein surface (F. Fraternali, personal communication), and these results will be published elsewhere. However, NOE contacts between the methyl groups of the BR label and the protein are not observed, and we do not observe any additional protection of main-chain hydrogen exchange for residues within helix C of troponin C, to which the rhodamine is attached.

A separate maximum entropy analysis of the TnC bifunctional rhodamine fluorescence measurements indicated a distribution of label orientations of approximately 26° on a longer time scale than the fluorescence lifetime.[10] The angular distribution reflected in the polarized fluorescence data from BR-TnC in muscle fibers must come from some other source, such as the movement of the domain to which the fluorophore is attached. This is consistent with NMR relaxation measurements on a troponin core complex.[34] In that study, the N-domain of TnC was seen to move independently from the core of the troponin complex when in the apo state. Taking the ratio of the ^{15}N-R_2 relaxation rates between apo and calcium-saturated forms of the troponin complex as an estimate of the order parameter S^2, the authors obtained $R_2^{apo}/R_2^{Ca} = 0.65-0.70$. Analysis of these results with a "wobble-in-a-cone" model,[21,35] where $S^2_{CONE} = [(1/2)\cos(\theta_o)(1 + \cos(\theta_o)]^2$, gave an angle of approximately 30° which agrees with the fluorescence analysis. Recently, Baber et al.[36] have applied a similar analysis to the motion of the two domains of calmodulin.

Conclusion

We have used NMR relaxation measurements to study the dynamics of a [^{13}C]methyl-labeled bifunctional rhodamine probe

(33) Gagné, S. M.; Tsuda, S.; Spyracopoulos, L.; Kay, L. E.; Sykes, B. D. *J. Mol. Biol.* **1998**, *278*, 667−686.
(34) Blumenschein, T. M.; Stone, D. B.; Fletterick, R. J.; Mendelson, R. A.; Sykes, B. D. *J. Biol. Chem.* **2005**, *280*, 21924−21932.
(35) Woessner, D. E. *J. Chem. Phys.* **1962**, *37*, 647−654.
(36) Baber, J. L.; Szabo, A.; Tjandra, N. *J. Am. Chem. Soc.* **2001**, *123*, 3953−3959.

attached to the C helix of the N-domain of troponin C and found no large range independent motion of the BR probe relative to the protein on a time scale shorter than the rotational correlation time of the TnC. This conclusion is in good agreement with fluorescence measurements which gave virtually identical order parameters for the motion of the dipole moment of the xanthene ring. The results presented herein support the utility of the overall bifunctional labeling strategy for determination of in situ protein domain orientations.

(37) ABBREVIATIONS: NOE, nuclear Overhauser effect; R_1, longitudinal relaxation rate, R_2, transverse relaxation rate; $R_{1\rho}$, spin lattice relaxation rate in the rotating frame; FID, free induction decay; TnC, troponin C; TnI, troponin I; $TnI_{115-131}$, switch peptide of TnI; sNTnC, N-domain of chicken skeletal troponin C; BR, bifunctional carborhodamine; sNTnC·$2Ca^{2+}$·$TnI_{115-131}$·BR_{56-63}, calcium saturated N-domain of skeletal troponin C with a BR probe attached to residues 56 and 63 of the C helix and bound to the switch peptide of TnI; CSA, chemical shift anisotropy; τ_t, correlation time for rotation of the methyl group around the three-fold symmetry axis; τ_s, internal correlation time for the $^{13}C-^{14}N$ bond; S^2_t, order parameter for methyl rotation; S^2_s, order parameter for motion of the $^{13}C-^{14}N$ bond; τ_m, isotropic macromolecular rotational correlation time; $\langle P_{2d} \rangle$, order parameter derived from fluorescence measurements describing the amplitude of the local rotation of the rhodamine dipole with respect to the protein backbone. Note that $\langle P_{2d} \rangle$ is an order parameter, whereas S^2 is the square of the order parameter.

Acknowledgment. We thank the Canadian National High Field NMR Centre (NANUC) for their assistance and use of the facilities. Operation of NANUC is funded by the Canadian Institutes of Health Research (CIHR), the Natural Science and Engineering Research Council of Canada (NSERC), and the University of Alberta. We thank Dave C. Corson for expression of the isotopic labeled protein and Roisean E. Ferguson for fluorescence labeling. We are grateful to Dr. David R. Trentham, Dr. Robert E. Dale, Dr. Franca Fraternali, and Professor Malcolm Irving for many helpful discussions. This work was supported by the CIHR. O.J. is the recipient of an Alberta Heritage Foundation for Medical Research (AHFMR) Studentship. L.S. is a AHFMR Senior Scholar.

JA0772694